Study of Polyethylene by Solid State NMR Relaxation and Spin Diffusion

R. R. Eckman, P. M. Henrichs,*,† and A. J. Peacock*

Exxon Chemical Company, 5200 Bayway Drive, Baytown, Texas 77520

Received November 8, 1995; Revised Manuscript Received January 14, 1997[⊗]

ABSTRACT: High-density polyethylene was studied by solid state ^{1}H NMR spectral fitting, relaxation, and spin diffusion methods. The results are compared with measurements made by Raman spectroscopy, solid state ^{13}C NMR, density, and DSC methods. A modified Goldman−Shen solid state ^{1}H NMR technique was used to estimate the thicknesses of microscopic domains of the polyethylene. Other information obtained is the mobility of polymer chains in the domains, the proton NMR spin diffusion rate constants, and the proton NMR spin−lattice relaxation times. Results indicate that the so-called interfacial phase of the polyethylene is significantly more dense than the amorphous phase and that transport of chains by the process called "chain diffusion" contributes to the mechanism of ^{1}H NMR spin−lattice relaxation.

Introduction

Semicrystalline polyethylenes are composed of domains with widely different polymer chain mobilities. In the crystalline domain the chains are highly ordered and can reorient only very slowly. These domains have a lamellar morphology. In the noncrystalline domains the polymer chains are more mobile. The degree of mobility of chains in the interlamellar noncrystalline polymer is a subject of much current interest, and it has been suggested that chains that are close to the lamellar crystalline surfaces are somewhat ordered and only moderately mobile.[1,2] Another portion of the noncrystalline polymer, more distant from the lamellae, is amorphous and composed of chains with high mobility.

Solid state ^{1}H NMR spectroscopy is sensitive to the different mobilities of the chains in solid polyethylene. The solid state ^{1}H NMR spectrum typically consists of overlapping peaks of very different width. Chains with high mobility contribute to the narrower peaks, and immobile chains in the crystalline domains contribute to the very broad peaks. By deconvolution of the spectrum, it is possible to determine the relative number of chains in these spatially distinct domains.

The Goldman−Shen solid state NMR technique has long been used to characterize the domain structure of semicrystalline polyethylenes.[3−6] This technique measures the course of diffusion of nuclear magnetization between the domains of the solid polymer, which include the crystalline, amorphous, and so-called interfacial regions.[1] Spin diffusion is the process by which nuclear magnetization is transported through a solid sample and from one domain to another as a result of flip−flop transitions due to the internuclear (^{1}H−^{1}H) dipole−dipole interactions. This process is distinct from a process involving transport of atoms in the sample, which might also cause a diffusion of nuclear magnetization. The microscopic dimensions of the polymer domains can be extracted from modeling of the spin diffusion process, and dynamic properties of the domains can be inferred. The domain size measurements complement knowledge obtained from Raman spectroscopy, X-ray, and electron diffraction, whereas the dynamic information obtained is unique to NMR. Goldman−Shen techniques have also been combined with multiple-pulse line narrowing[7−9] and ^{13}C detection methods.[10−13]

In this note we measure the domain structure, chain dynamics, and crystallinity of polyethylene by analysis of proton spin diffusion and spin−lattice relaxation. A modified Goldman−Shen technique is used and the results are compared to those obtained with several other methods.

Solid State ^{1}H NMR of Polyethylene

The solid state ^{1}H NMR spectrum of polyethylene consists of a narrow signal with a width of about 10 kHz from protons in the noncrystalline domains, overlapping a broad signal with a width of as much as 70 kHz from protons in the crystalline domains.[14−19] Also, there usually appears to be a smaller signal having a width between those two values.[16,18,20,21]

Crystallinity of polyethylene can be measured with NMR by two approaches. First, deconvolution of the spectrum can give the integrated intensities of the three types of signals: broad, intermediate, and narrow. When a two-component fit is used, i.e., broad and narrow components, the fraction of the total intensity that the broad signal represents is usually slightly higher than the crystallinity measured by X-ray diffraction.[20,22,23] Although most of the broad signal comes from protons in the crystalline portions of polyethylene, it is believed that some of the chains in the noncrystalline regions of polyethylene are actually relatively immobile and contribute also to the broad and intermediate signals.[20] Satisfactory agreement with the X-ray measurement is usually obtained with a three- or four-component fit of the NMR spectrum,[14,16,20,21] but unambiguous fitting of the spectrum with three or more components is not generally possible. One problem is that the overlapping peaks are difficult to distinguish. Another is that some of the intensity of the broad signal is lost in the spectrum when either single-pulse or spin-echo detection is used. Single-pulse detection requires a preacquisition delay, which decreases the intensity of the broad signal more than the narrow signal. Spin-echo detection gives the same problem since it does not completely refocus the signal of the broad component.[24]

The second approach involves analysis of the solid state ^{1}H NMR spin−lattice relaxation curves. For the typical solid polymer the return of nuclear magnetization to equilibrium following an rf pulse is faster for the

† Present address: Nycomed Research and Development, 466 Devon Park Drive, Wayne, PA 19087.

[⊗] Abstract published in *Advance ACS Abstracts,* March 15, 1997.

S0024-9297(95)01675-5 CCC: $14.00

chains of higher mobility than for those of lower mobility. Computer fitting of the course of nuclear relaxation allows deconvolution of the decay curve into parts associated with the crystalline and noncrystalline regions.[25,26] However, this deconvolution can be ambiguous due to the difficulty of fitting multiexponential curves.

Measurements of crystallinity in polyethylene with these two approaches usually differ because they depend on quite different spin physics.[27−29]

Measurement of Spin Diffusion

The deconvolution techniques described above measure only the quantity of protons in a polymer domain. The spin diffusion technique actually determines the microscopic dimensions of the polymer domains and provides information about the dynamic properties of the chains in those domains. The distance measurement is obtained from computer fitting of a relaxation curve that is sensitive to spin diffusion.[23,30−33] In the absence of spin diffusion, the nuclear magnetization of each domain would decay at its characteristic rate determined mainly by the mobility of polymer chains in each domain. However, spin diffusion modifies the relaxation rates of each of the various domains that it affects. Analysis of the effect of spin diffusion on the course of nuclear spin−lattice relaxation provides information about the physical dimensions of the domains.[34,35] Interpretation of the line widths and nuclear relaxation rates gives information about chain mobility.

In order for net magnetization transfer between two domains as a result of spin diffusion to occur, the magnetization levels of the two domains must differ. To generate the differences, two elegant methods have been devised. First, the Goldman−Shen[3] sequence prepares the system selectively so that longitudinal magnetization exists only for the protons in the domains giving the narrow peak. Magnetizations for the other domains are zero. The reappearance of magnetization in the domains giving the broad peak over the course of the experiment indicates that spin diffusion has taken place. In the second experiment, the Packer sequence[29] prepares the system in the reverse initial state with magnetization only in those domains giving rise to the broad NMR signal. Spin diffusion reintroduces magnetization into the domains giving the narrow signal during the course of this experiment.

A limitation of these experiments is that the difference between the magnetizations of the two domains that can be prepared is limited. This is because in nulling the magnetization of one of the components, most of the magnetization of the other component is sacrificed. This means that the total initial signal measured is small and the signal-to-noise ratio is low. Also, spin−lattice relaxation occurring along with spin diffusion partially obscures the course of spin diffusion.

Modified Goldman−Shen sequences have been proposed to reduce spin−lattice relaxation effects in the measurement of spin diffusion.[36,37] We have used the pulse sequence of Zhang and Mehring[38,39] with a final pulse for generation of a solid echo to obtain relaxation curves for polyethylenes. We find that these modified relaxation curves have useful features, i.e. the effects of spin diffusion are more easily observed and thus they offer some advantage over previous methods for detection of spin diffusion.

The modified experimental pulse sequence is shown in Figure 1. It consists of a Goldman−Shen preparation

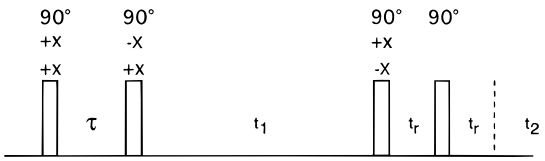

Figure 1. Goldman−Shen pulse sequence with a final pulse to refocus a spin echo.

period, τ, followed by a spin diffusion period, t_1. The final pulse refocuses a solid echo during the time $2t_r$, and the signal is detected during t_2.

The refocusing time t_r for the spin echo that we used was 15 μs. For a refocusing time of this length the echo is substantially attenuated relative to the initial signal.[24] The signal attenuation is greater for the broad component than the narrow component. The differential loss between the two types of signals must be taken into account as a fitting parameter when the results are analyzed.

The signals generated by pulses with the phases shown on the first line of Figure 1 were added to those generated by pulses with the phases shown on the second line. Detection of a difference magnetization in this manner has the advantage that it is known in advance to have the value zero for long t_1 and need not be treated as a fitting parameter in the analysis. Furthermore, alternation of the pulse phases helps to eliminate spectral artifacts. The phase alternation used here is similar to that of Torchia sequence, which is widely used for measurement of spin−lattice relaxation times in solids.[40] Additional phase cycling was also imposed; we used $1 = \{8(+x)\}$, $2 = \{4(-x)4(+x)\}$, $3 = \{+x,-x,+x,-x,-x,+x,-x,+x\}$, $4 = \{2(-y,-y,+y,+y)\}$, and $R = \{2(+,-,+,-)\}$ for the phases of the four pulses and the receiver.

The paths of the magnetization vectors, M_b and M_n, corresponding to broad and narrow spectral components, respectively, during the experiment of Figure 1 are illustrated in Figure 2. Initially, the vectors are aligned along the $+z$ axis of the rotating frame, in the direction of the external magnetic field. The first pulse rotates both of them to the $+y$ axis. M_b decays more rapidly than M_n, and the delay τ is chosen such that M_b is just zero at its end. A good value for polyethylene was 28 μs. The remaining portion of the vector M_n is rotated back to the $+z$ axis after τ by the second pulse. This is the Goldman−Shen selection.

In the absence of spin diffusion, M_n and M_b would decay as single exponentials during t_1 with the eight-scan phase cycle used. The magnetization represented by M_n, when measured after t_1, would be $1 + \{M_{n,0}[\exp(-\tau/T_{2,n})] - 1\}[\exp(-t_1/T_{1,n})]$ for the first four scans and $-1 - \{-M_{n,0}[\exp(-\tau/T_{2,n})] - 1\}[\exp(-t_1/T_{1,n})]$ for the second four scans; where $M_{n,0}$ is the equilibrium value of M_n, $T_{1,n}$ is the intrinsic spin−lattice relaxation time constant of M_n, and $T_{2,n}$ is the intrinsic spin−spin relaxation time constant of M_n. Thus for eight scans the magnetization $M_n = 2\{M_{n,0}[\exp(-\tau/T_{2,n})][\exp(-t_1/T_{1,n})]\}$. A similar equation holds for the magnetization represented by M_b in the absence of spin diffusion. Also, when measured after t_1, M_b would be zero for $\tau \gg T_{2,b}$.

The effect of spin diffusion is to connect M_n and M_b during t_1 so that their evolution is not simple exponential. In fact, M_b is zero when $t_1 = 0$ and $\tau \gg T_{2,b}$. Yet M_b actually increases during the early part of t_1 as a portion of M_n is converted into M_b by spin diffusion. Consequently, M_n decreases rapidly during the early part of t_1 since it is converted into M_b. It is these

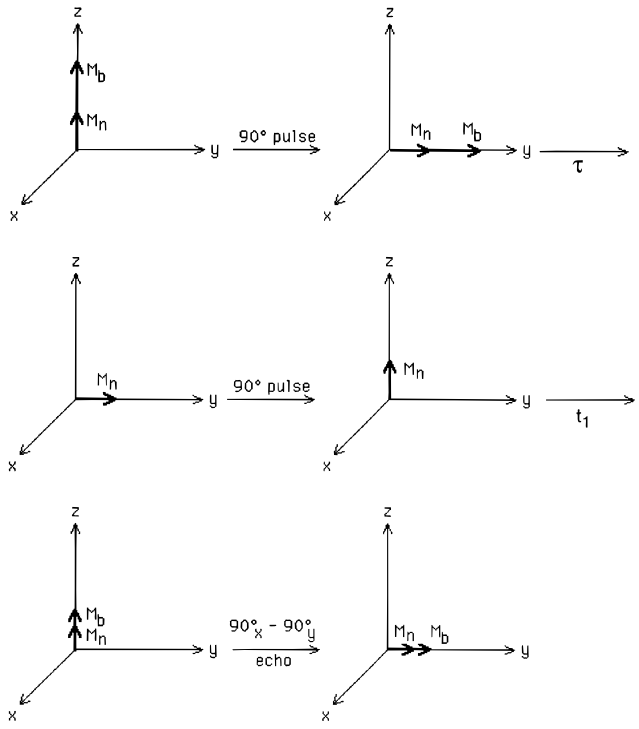

Figure 2. Path of the nuclear magnetization vectors corresponding to a narrow spectral component, M_n, and a broad component, M_b, in the modified Goldman−Shen pulse sequence of Figure 1.

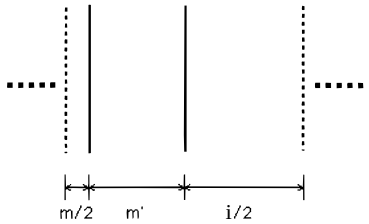

Figure 3. One-dimensional model for solid polyethylene. The chains in the regions m and m' are mobile enough that their ^{1}H NMR spectrum is narrowed, whereas the chains in the region i are immobile and their spectrum is broad.

features which are more readily observed in the modified Goldman−Shen sequence. Matching these features with calculated curves enhances the fitting and thus the measurement of spin diffusion.

Theoretical Basis for the Data Analysis

The experimental decay curves were compared to theoretical curves calculated for the one-dimensional structural model illustrated in Figure 3. Since polyethylene has a semicrystalline lamellar structure, the model is taken as a repeating series of crystalline and noncrystalline regions. The repeat unit of the model structure has three different regions: a region i of length l_i in which the polymer chains are immobile and contribute to the broad spectral component, a region m' of length $l_{m'}$ in which the polymer chains are somewhat mobile and contribute to the narrow spectral component, and a region m of length l_m in which the polymer chains are quite mobile and also contribute to the narrow spectral component. The intrinsic spin−lattice relaxation time, T_1, in the absence of spin diffusion of the protons was assumed to be uniform within each region. Thus three T_1's were assigned: $T_{1,i}$ which is long, $T_{1,m'}$ which is somewhat shorter, and $T_{1,m}$ which is short. Note that we propose that the mobility of polymer chains in region m' is great enough to narrow the spectrum of protons in m' (as compared to the crystalline region), but not so great as to make $T_{1,m'}$ very short (as expected in the amorphous region).

The basic repeat unit was subdivided into 20 discrete sections or slices of equal length. The magnetization level in the various sections was then represented by the elements of a vector **M**. The complete list of parameters needed to describe the model are the number of sections, the lengths of the regions, the spin−lattice relaxation rate of each section, the rate at which magnetization is transferred among the slices, and the initial vector $\mathbf{M}(t=0)$.

The rate of change of **M** due to spin diffusion and spin−lattice relaxation is expressed by

$$d\mathbf{M}(t)/dt = \mathbf{A}\cdot\mathbf{M}(t) \quad (1)$$

where **A** is a 20 by 20 matrix.

The off-diagonal element $A_{i,i+1}$ of **A** represents the rate at which magnetization moves from section $i + 1$ into i. Likewise, the element $A_{i-1,i}$ gives the rate at which magnetization travels from section $i - 1$ into i. All four off-diagonal elements of **A** are zero. The diagonal elements are restricted by the off-diagonal elements to the values $A_{i,i} = -A_{i-1,i} - A_{i,i+1} - R_i$, where R_i is the rate of spin−lattice relaxation of section i. The boundary conditions are that elements $A_{1,1} = -A_{1,2} - R_1$ and $A_{20,20} = -A_{19,20} - R_{20}$. The rate at which magnetization is transferred between sections at the interface of two polymer regions was assumed to be the average of the rate of magnetization transfer between sections within each of the regions separately.

The formal solution of eq 1 for **M** is

$$\mathbf{M}(t) = \exp(\mathbf{A}t)\cdot\mathbf{M}(t=0) = \mathbf{D}^{-1}\exp(\mathbf{E}t)\cdot\mathbf{D}\cdot\mathbf{M}(t=0) \quad (2)$$

The matrices **D** and $\mathbf{D}^{-1}$ are those that diagonalize **A**, and **E** is a diagonal matrix containing the eigenvalues of **A**.

At the start of the fitting, solutions for **M** with various initial conditions were calculated and compared by eye to the experimental results. As indicated below, some parameters were found to be insensitive to the experimental results and were set to assumed values. Then the remaining parameters were set free to be adjusted by the computer for the best fit.

Experimental Section

The modified Goldman−Shen experiments were performed on a sample of high-density polyethylene, Phillips Marlex 6009, that had been quenched in ice water from the melt (IWQ sample). The number average molecular weight was 150 000 and the molecular weight polydispersity was $M_w/M_n = 12.5$. The percent crystallinity as measured by Raman spectroscopy, density, and differential scanning calorimetry (DSC) were 66, 71, and 62%, respectively.[41,42] The lamellar thickness measured by Raman spectroscopy was 178 Å. Density was measured with a gradient column using triethylene glycol and 2-propanol.

NMR experiments were performed on a Bruker MSL 400 spectrometer operating at $\omega_0/2\pi(^1\text{H}) = 400.13$ MHz. The ^{1}H NMR probe had a 5 mm coil and a 90° pulse time from 1.7 to 2.1 μs. The time t_r for echo formation in the spin diffusion experiment was 15 μs. A delay of 9−10 s was used between scans. This value allowed complete return of the broad and narrow signals to equilibrium. The sequencing of the delay times t_1 in the experiment was also randomized to reduce artifacts in the relaxation curves. In the experiment with $\tau =$ 28 μs, the acquisition time per t_1 delay was about 3 h to give

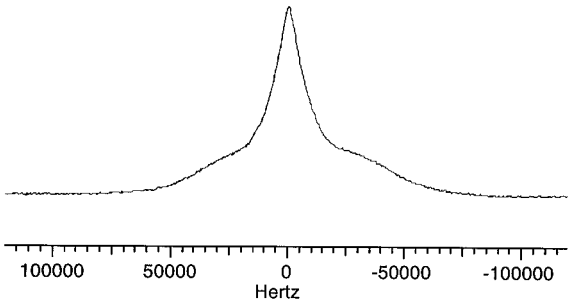

Figure 4. Solid state ^{1}H NMR spectrum of ice-water−quenched high-density polyethylene (Marlex 6009).

good signal to noise. All results were obtained at ambient temperature, about 22 °C.

Solid state ^{1}H NMR spin−lattice relaxation times (T_1) were also measured with the same probe by inversion recovery on three samples: (a) the IWQ sample, (b) the same polymer isothermally crystallized for 16 days at 128.5 °C (16d sample), and (c) the same polymer crystallized by slow cooling in air from the melt (SC sample).

Elaborate procedures are available for deconvolution of the solid state proton NMR spectrum of polyethylene into its basic components.[14,17,21,43] In this work it was sufficient to deconvolute spectra by fitting the polyethylene spectrum to the sum of a narrow Lorentzian signal with a full width at half-maximum of 10.3 kHz and a broad Gaussian signal with a full width at half-maximum of 68.1 kHz. The relative fraction that the broad signal represented was taken as the crystallinity of the sample. For the spin diffusion experiments, two decay curves, corresponding to the broad and narrow spectral components, were generated by deconvolution from a single set of data. The least-squares fitting of the solid state ^{1}H NMR spectrum was done with the curve fitting module of NMR1, supplied by New Methods Research, Inc., using a DEC μVaxII workstation.

Theoretical fits to the proton relaxation decay curves generated with the modified Goldman−Shen method of Figure 1 were calculated with an iterative least-squares Gauss−Newton algorithm. The program for the calculation was written with Mathematica V2.03E and executed on a Macintosh IIfx PC. The error analysis was done with standard methods.[44] Calculation times for the complete iteration depended on the error limits chosen. Typically, a few hours were required to obtain optimum fits.

Results of Modified Goldman−Shen Experiment

The solid state ^{1}H NMR T_1 measured by inversion recovery for the three samples were 16d sample, 4.5 s; SC sample, 2.7 s; IWQ sample 1.9 s.

The solid state ^{1}H NMR spectrum of the IWQ sample of polyethylene measured with a solid echo is shown in Figure 4. This spectrum was fit to a broad component comprising 66% of the total area and a narrow component comprising 34%. Thus the percent crystallinity as measured by NMR was 66%.

The relaxation curves obtained from the modified Goldman−Shen experiment of Figure 1 with delay $\tau = 1$ μs are shown in Figure 5. Figure 5a shows the decay of the total magnetization. The data points in Figure 5, b and c, represent the relative integrated intensities of the narrow and broad spectral components, respectively. The dots on the curves are the experimental data points, and the solid lines are the calculated curves that are described in detail in the Discussion section. Since the delay τ was short for the curve of Figure 5a, the result was nearly the same as for an inversion-recovery measurement with the Torchia method.[40] The total equilibrium magnetization was taken as unity; thus the first point in Figure 5a was set to 1.0. The first point in Figure 5b was 0.34 of the total magnetization, and

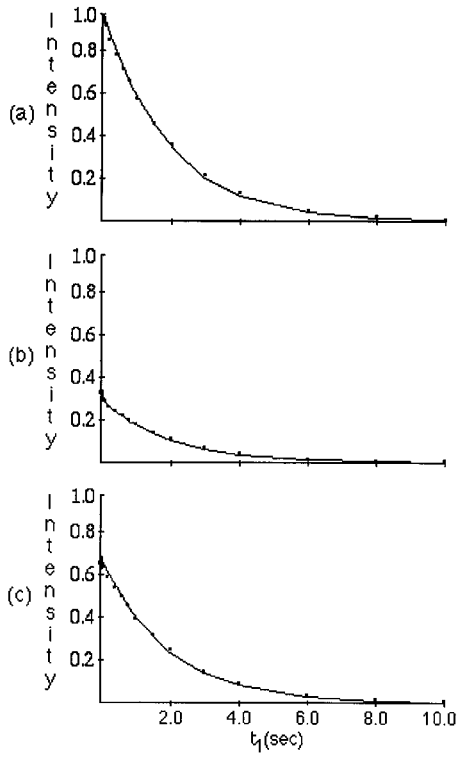

Figure 5. Relaxation curves for the modified Goldman−Shen experiment with $\tau = 1$ μs: (a) total magnetization; (b) narrow spectral component; (c) broad spectral component.

the first point in Figure 5c was 0.66 of the total magnetization. As expected, these initial magnetizations were the same as that found in Figure 4, since all were measured with a solid echo under the same conditions.

Note that both the broad and narrow components of Figure 5 decay in a similar fashion to the total magnetization. The curve of Figure 5a for the total magnetization was fit to a single exponential to give a time constant of $T_1 = 1.9$ s, the same value found by inversion recovery.

The relaxation curves obtained from the modified Goldman−Shen experiment of Figure 1 with delay $\tau = 28$ μs are shown in Figure 6. The data shown were processed in the same way as those for Figure 5. With the delay $\tau = 28$ μs the initial magnetizations were zero for the broad component and 0.45 for the narrow component, and the first point in Figure 6a was (0.45)(0.34) = 0.15. Thus, in the initial state for this experiment, only 0.15 of the total equilibrium longitudinal magnetization of the narrow component remained. This was the maximum difference in magnetization between the broad and narrow components that we could prepare.

The most striking features of the data shown in Figure 6 are the rapid decay of signal at the beginning of curves a and b and the rapid increase in intensity in curve c. These effects are due to spin diffusion. The rapid increase in intensity in curve c is a clear demonstration of the return of magnetization to the broad spectral component via spin diffusion after Goldman−Shen preparation. The spectrum obtained at $t_1 = 0.2$ s in the experiment of Figure 6 is shown in Figure 7. At this point in the evolution, the narrow signal has become small enough so that the reappearance of the broad signal is unmistakable.

The model proposed in Figure 3 for the solid state polymer structure of polyethylene is critical to the

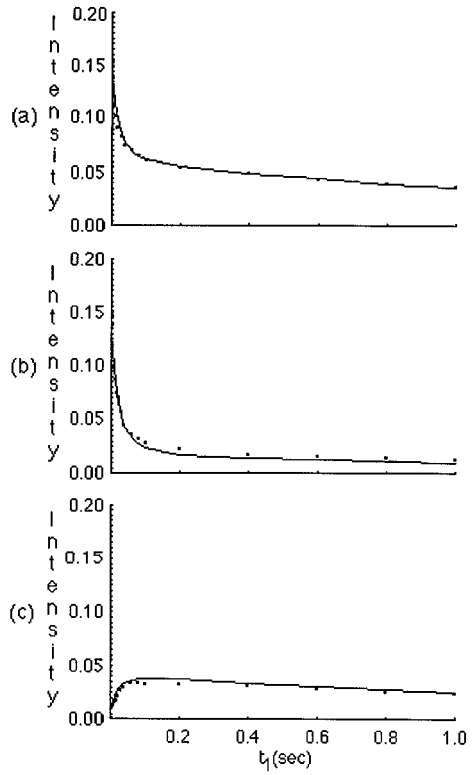

Figure 6. Relaxation curves for the modified Goldman−Shen experiment with $\tau = 28\ \mu$s. Note the difference in the scale of the horizontal axis from the plots of Figure 5.

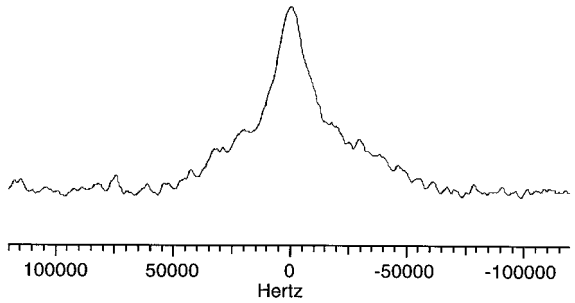

Figure 7. Solid state ^{1}H NMR spectrum of Marlex polyethylene obtained at $t_1 = 0.2$ s in the experiment with $\tau = 28\ \mu$s.

interpretation of the experiments. We found that this model, with three domain types, could be used to fit simultaneously the curves for both long and short values of τ with the parameters shown in Table 1. The calculation was insensitive to the intrinsic T_1 for region *i*. It only needed to be at least some 3−4 s. This is longer than the intrinsic T_1 found for region *m′* and longer than the time required for magnetization to traverse the crystalline region by spin diffusion. For a crystal thickness of 200 Å and $D = (3-6) \times 10^{-16}$ m^2/s, the time required to traverse the crystal[7] would be about $t = [3/(4D)](200 \times 10^{-10})^2 \sim 0.5-1$ s. The calculation was also insensitive to the spin diffusion rate in region *m*, although it was restricted to a relatively small value by the model (a region with very mobile chains must have a small spin diffusion rate). The values in boldface in Table 1 are the results generated by the iterative fitting: the thicknesses of the three regions, the spin diffusion rate constant for region *m′*, and the intrinsic T_1 of regions *m* and *m′*.

While the values for initial magnetization do represent quantities fit to the experimental data and are necessary for the calculation, there is little to be inferred from their resulting value. The initial magnetizations

Table 1. Parameters for Best Fit of Model to the NMR Results for the IWQ Marlex[a]

parameter	region *m*	region *m′*	region *i*
thickness (Å)	**24**	**49**	**221**
intrinsic T_1 (s)	**0.143**	**2.76**	1000[c]
spin diffusion rate const (m^2/s)	0[c]	**1.1×10^{-16}**	3.1×10^{-16}[b]
initial magnetization			
$\tau = 1\ \mu$s	1.0[c]	1.0[c]	1.2[d]
$\tau = 28\ \mu$s	0.75[c]	0.35[c]	0.001[c]
signal scaling[e]	1.0	1.0	0.42

[a] Model shown in Figure 3. [b] Calculated values not iterated (see text). [c] Assumed values not iterated. [d] See text. [e] Accounts for loss of signal during formation of the spin echo.

shown in Table 1 were the fraction of the individual magnetization remaining for each region after the Goldman−Shen preparation, i.e., after τ. This should be unity for each region when $\tau = 1\ \mu$s and less than unity for longer τ. In the calculation, all initial magnetizations were allowed to be iterated and the values rapidly settled to those shown in Table 1. These values were then fixed and the iteration continued to find the remaining parameters.

One problem was that the calculation generated an initial magnetization of region *i* when $\tau = 1\ \mu$s greater than unity, apparently because some of the broad signal is lost in forming the spin echo. Thus, for the best fit, the iteration wanted to have extra initial magnetization in region *i*. This problem may also be due to the limited number of slices used in the calculation.

The calculation generated initial magnetizations of 0.75 for region *m* and 0.35 for region *m′*. Thus, the calculation distributed the initial experimentally measured magnetization for the narrow component (which contains signals from both regions) between those two regions.

In the past it has been difficult to measure spin diffusion because the Goldman−Shen relaxation curves decreased monotonically. This was mainly because spin diffusion only transferred magnetization, while the total signal remained constant. Since there was also a steady loss due to spin−lattice relaxation, the curves were not very sensitive to the calculated models. The curves of the modified Goldman−Shen experiment (see Figure 6) exhibited a very rapid change in the beginning and a long tail. This shape was more sensitive to calculated models, since both these features must be reproduced by the calculation. The rapid decay of M_n at the start of the modified Goldman−Shen curve is partly due to the detection of the signal with a spin echo. Magnetization which is initially only in the narrow peak is transferred to the broad peak. However, the broad peak is not detected at full intensity but is scaled by a factor 0.42. Thus the transfer by spin diffusion results in a net loss of observed signal and a rapid decay in the beginning. This is a key factor that enhances the measurement of spin diffusion.

It was critical to observe the growth of M_b and the decay of M_n at small t_1 values for $\tau = 28\ \mu$s to measure the effect of spin diffusion by fitting the curves. The signal to noise at that point depended on the term $\exp(-\tau/T_{2,n})$, which determined the size of M_n when $t_1 = 0$. Thus the choice of τ was critical to the results. Since the maximum value that M_b attained was only some 3−4% of the total magnetization, τ must be at least 5 times longer than $T_{2,b}$ so that M_b is initially very close to zero. We estimate for the narrow signal, $T_2 \approx 1/(\pi \times 10.3 \times 10^3) = 31\ \mu$s and $\exp(-28/31) = 0.40$, which is

close to the measured initial M_n of 0.45. For the broad signal, $T_2 \approx 1/(\pi \times 68.1 \times 10^3) = 4.7$ μs and $\exp(-28/4.7) = 0.003$, which is small enough that it did not interfere with measurement of the growth of M_b via spin diffusion. Also, the free induction decay for a broad Gaussian peak decays to zero at 28−30 μs for a fwhm of 68 kHz.[45] The baseline of the spectrum observed at $t_1 = 0$ was quite flat and no broad signal was seen. If a longer value of τ was used, the experiment quickly became difficult to interpret due to low signal to noise. In our experience, it was not possible to obtain reasonable curves for a value of τ greater than about 36−40 μs.

Discussion and Results for Polyethylene

It has long been known that polyethylene contains an amorphous component and a crystalline component. The work described here provides evidence for fast spin diffusion between the components of polyethylene and makes possible a quantitative measure of the sizes of the crystalline domains and clarification of their chemical nature.

Amorphous polyolefins or hydrocarbons with high molecular mobility typically have a ^{1}H spin−lattice relaxation time constant, T_1, at room temperature of less than 1 s due to the rapid molecular motions. For example, noncrystalline ethylene−propylene copolymers and many elastomers have T_1's much less than 1 s.[46] Crystalline solids with little internal molecular motion have long T_1's, usually much larger than 1 s. Thus, in the absence of spin diffusion, one would expect to observe biexponential relaxation, i.e., two independent T_1 values, in semicrystalline polyethylene. The fact that a single T_1 is observed for solid polyethylene has long been assumed to be indirect proof that spin diffusion in polyethylene is rapid.[23,30−32] However, the averaging of the spin−lattice relaxation rates by spin diffusion obscures the intrinsic values of the rates in the absence of spin diffusion. In fact, partially relaxed spectra from an inversion recovery experiment showed that the broad peak can be inverted while the narrow peak is not, thus suggesting that their intrinsic T_1's are different.

The results shown here provide evidence that the T_1 of at least some of the protons in the amorphous region of polyethylene at room temperature is much less than 1 s. Protons having such short relaxation times must be located in highly mobile polymer chain units, most likely unencumbered by chain entanglements or by interactions with the crystalline lamellae. Thus, in future work the measurements might be able to differentiate between entangled chain units and the remainder of the amorphous region.

Models with only two domains were inadequate for fitting the experimental data obtained in this work. Likewise, three-phase models with two of the phases corresponding to the broad NMR signal were insufficient. A good fit was only obtained with a region m' that contributes to the narrow signal. Nevertheless, the three-domain model with two domains contributing to the narrow NMR signal is probably a minimal model for interpretation of the data since there are probably at least four dynamically different types of chains in polyethylene when entanglement points in the amorphous region are considered. In further discussion we assign region i to the crystalline domain, region m' to the so-called interfacial domain, and region m to the amorphous domain.

A means for observation of spin diffusion in polymers such as polyethylene is useful in the extraction of quantitative information that can be related to the details of solid state polymer structure. In theory, even if spin diffusion were to take place between only two different domains of a solid, the relaxation curve would be composed of an infinite number of exponential components.[31,32] Separation of such an experimental curve into its several component exponential parts is known to be difficult,[32,47−53] and interpretation of the various exponentials is subject to ambiguity even if they can be extracted.

Table 2. Solid State NMR T_1's (s) of Marlex Polyethylenes

sample	^{13}C T_1[a]	^{1}H T_1[b]
IWQ	895, 40, 0.6	1.9
SC		2.7
16d	2990, 132, 0.4	4.5

[a] The three time constants found in a three-exponential fit of relaxation curves obtained with the Torchia method.[40] [b] Measured by inversion-recovery, single exponential fit.

In fitting the experimental relaxation curves, the spin diffusion constant used for the crystalline region was 3.1×10^{-16} m^2/s, a value calculated from the spectral width.[30] The spin diffusion constant found by fitting for the interfacial region was 1.1×10^{-16} m^2/s. By the same calculation, this corresponds to a line width of 22 kHz, significantly larger than that used to fit the NMR data. Thus it suggests that reduced mobility is found in the interfacial region.

The spin diffusion rate in the most mobile phase, region m, was set to zero. The presence of relatively slow spin diffusion within region m in the model and the thickness of region m had essentially no effect on the fitting of the curves. In other words, spin diffusion in region m was not needed in the model. This agrees with our expectation that chains in the amorphous region are highly mobile, that the residual secular proton dipolar couplings are small, and that the proton T_1 of this region is small. An interesting interpretation of this result is that a narrow slice of region m acts as the spin−lattice magnetization sink for the adjacent regions of lesser mobility. This slice can represent an interface of only a few to several angstroms thickness. A uniform T_1 for the rest of region m would then be found due to the reorientation, exchange, and transport dynamics of the chains in that region.

The simple model of Figure 3 has significant weaknesses in explaining ^{1}H spin relaxation processes in polyethylenes. First, it is only one-dimensional. Second, it does not include molecular dynamics such as chain transport, one mode of which for polyethylene is called "chain diffusion".[54] On the time scale of selective Goldman−Shen experiments, about 1 s, it has been shown that the diffusion of chains between the regions of the polymer is significant, possibly as much as 100 repeat units. Thus magnetization can be transported by chain diffusion, as opposed to spin diffusion, and having an intrinsic T_1 for each region may not be an adequate description. Spin diffusion ($D \approx 10^{-16}$) is probably more rapid than chain diffusion ($D \approx 10^{-17}$−10^{-21}) in the regions of lesser mobility at room temperature.[54] Chain diffusion has been shown to cause the dependence of solid state ^{13}C NMR T_1 on lamellar thickness.[54] In our samples, we note that the solid state ^{1}H NMR T_1 also increases as the crystallinity and lamellar thickness increase. The ^{1}H and ^{13}C NMR T_1's for the samples are recapitulated in Table 2. The T_1 results suggest that chain diffusion or exchange dynamics also plays a role in the ^{1}H NMR spin relaxation. The

Table 3. Crystallinity of Marlex Polyethylenes (wt %)

sample	solid state ^{1}H NMR	Raman[a]	density	DSC
IWQ	66	66	71	62
		14		
		22		
SC		75	81	68
		7		
		17		
16d	86	87	90	82
		3		
		10		

[a] From top to bottom, these correspond to the crystalline, interfacial, and amorphous regions, respectively.

lamellar thickness for the 16d sample was about 325 Å by Raman. If chain diffusion dominates the mechanism of relaxation, then the T_1 of the 16d sample would be about $(325/178)^2 = 3.3$ times that of the IWQ sample.[54] The ratio we observed was 2.4 for ^{1}H and 3.3 for ^{13}C. Evidently, the chain diffusion mechanism dominates the ^{13}C relaxation and should be a part of the modeling of proton NMR relaxation in solid polyethylene. This could be corroborated by studies of the temperature dependence of T_1 and the rate of spin diffusion, and study of the spin diffusion in the 16d sample.

According to the results of Axelson, the ^{13}C $T_1 = 895$ s of the IWQ Marlex corresponds to a lamellar thickness of about 220 Å.[55] This is compared to results found in this work: Raman, 178 Å; and ^{1}H NMR spin diffusion (Table 1), 221 Å. The ^{13}C $T_1 = 2990$ s of the 16d Marlex corresponds to a lamellar thickness of about 490 Å, significantly higher than measured by Raman, 325 Å.

It is interesting to compare the results of the measurement of crystallinity of the polyethylene by different methods, which are recapitulated in Table 3. The uncertainty in all values for crystallinity in Table 3 is about ±5 or less, so that solid state ^{1}H NMR and DSC gave essentially the same result. A trend is that density gave a value significantly higher than the other methods. The value for crystallinity obtained from density measurements is larger because it is essentially a measure of the crystalline and interfacial content. Thus the results indicate that the interfacial region is significantly more dense than the amorphous region.[56] Furthermore, the solid state spin diffusion NMR experiment indicates that the mobility in the interfacial region is great enough to substantially narrow its proton NMR spectrum.

The modified Goldman−Shen experiment of Figure 1 is useful for measurement of the thicknesses of regions i and m', as well as the rate of spin diffusion. The thickness of the interfacial region, m', in Table 1 was 49 Å. This represents some 20 repeat units for an all-trans chain. If the densities of the crystalline and interfacial regions are similar, then the ratio of weights as measured by Raman (Table 3), 66%/14% = 4.7, agrees with the ratio of the thicknesses as measured by NMR, 221 Å/49 Å = 4.5. Of course, the thickness measured by NMR is dependent on the model chosen to represent the morphology of the polymer.

In future, details of polymer morphology and heterogeneity may be investigated by novel proton spin diffusion methods.[57] The techniques may also be useful for studies of solid polypropylene at elevated temperature where the proton spectrum exhibits broad and narrow components.

Acknowledgment. The authors are grateful to Professor Leo Mandelkern for sample preparation at Florida State University and for critical reading of the manuscript. We thank Sandra Wapp for expert technical assistance.

References and Notes

(1) Fedotov, V. D.; Schneider, H. Structure and Dynamics of Bulk Polymers by NMR-Methods. In *NMR Basic Principles and Progress*; Diehl, P., Fluck, E., Gunther, H., Kosfeld, R., Seelig, J., Eds.; Springer-Verlag: New York, 1989; Vol. 21.
(2) Mark, J. E.; Eisenberg, A.; Graessley, W. W.; Mandelkern, L.; Samulski, E. T.; Koenig, J. L.; Wignall, G. D. *Physical Properties of Polymers*, 2nd ed.; American Chemical Society: Washington DC, 1993.
(3) Goldman, M.; Shen, L. *Phys. Rev.* **1966**, *144*, 321.
(4) Assink, R. A. *Macromolecules* **1978**, *11*, 1233.
(5) Cheung, T. T. P. *J. Chem. Phys.* **1982**, *76*, 1248.
(6) Cheung, T. T. P.; Gerstein, B. C. *J. Appl. Phys.* **1981**, *52*, 5517.
(7) Havens, J. R.; VanderHart, D. L. *Macromolecules* **1985**, *18*, 1663.
(8) Caravatti, P.; Neuenschwander, P.; Ernst, R. R. *Macromolecules* **1986**, *19*, 1889.
(9) VanderHart, D. L. *Makromol. Chem., Macromol. Symp.* **1990**, *34*, 125.
(10) Schmidt-Rohr, K.; Clauss, J.; Blumich, B.; Spiess, H. W. *Magn. Reson. Chem.* **1990**, *28*, S3.
(11) Newman, R. H. *Chem. Phys. Lett.* **1991**, *180*, 301.
(12) Kimura, T.; Neki, K.; Tamura, N.; Horii, F.; Nakagawa, M.; Odani, H. *Polymer* **1992**, *33*, 493.
(13) Spiegel, S.; Schmidt-Rohr, K.; Boeffel, C.; Spiess, H. W. *Polym. Commun.* **1993**, *34*, 4566.
(14) Kitamaru, R.; Horii, F. *Adv. Polym. Sci.* **1977**, *26*, 137.
(15) Bergmann, K.; Nawotki, K. *Kolloid Z. Z. Polym.* **1967**, *219*, 132.
(16) Bergmann, K. *Ber. Bunsenges. Phys. Chem.* **1970**, *74*, 912.
(17) Bergmann, K. *J. Polym. Sci., Polym. Phys. Ed.* **1978**, *16*, 1611.
(18) Kitamaru, R.; Horii, F.; Hyon, S.-H. *J. Polym. Sci., Polym. Phys. Ed.* **1977**, *15*, 821.
(19) Doskocilová, D.; Schneider, S.; Jakes, J.; Schmidt, P.; Baldrian, J.; Hernández-Fuentes, I.; Alonso, M. C.; Caceres, M. *Polymer* **1986**, *27*, 1658.
(20) Bergmann, K.; Nawotki, K. *Kolloid Z. Z. Polym.* **1972**, *250*, 1094.
(21) Phaovibul, O.; Loboda-Cackovic, J.; Cackovic, H.; Hosemann, R. *Makromol. Chem.* **1974**, *175*, 2991.
(22) Bergmann, K. *Kolloid Z. Z. Polym.* **1973**, *251*, 962.
(23) Kauffman, J. S.; Dybowski, C. *J. Polym. Sci., Polym. Phys. Ed.* **1989**, *27*, 2203.
(24) Rhim, W. K.; Pines, A.; Waugh, J. S. *Phys. Rev. B* **1971**, *3*, 684.
(25) Fedotov, V. D.; Ebert, A.; Schneider, H. *Phys. Stat. Solidi (a)* **1981**, *63*, 209.
(26) McBrierty, V. J.; Douglass, D. C. *Phys. Rep.* **1980**, *63*, 61.
(27) Bergmann, K. *Polym. Bull.* **1981**, *5*, 355.
(28) Fujimoto, K.; Nishi, T.; Kado, R. *Polym. J.* **1972**, *3*, 448.
(29) Packer, K. J.; Pope, J. M.; Yeung, R. R.; Cudby, M. E. A. *J. Polym. Sci., Polym. Phys. Ed.* **1984**, *22*, 589.
(30) Cudby, M. E. A.; Packer, K. J.; Hendra, P. J. *Polym. Commun.* **1984**, *25*, 303.
(31) Kenwright, A. M.; Packer, K. J.; Say, B. J. *J. Magn. Reson.* **1986**, *69*, 426.
(32) Booth, A. D.; Packer, K. J. *Mol. Phys.* **1987**, *62*, 811.
(33) Colquhoun, I. J.; Packer, K. J. *British Polym. J.* **1987**, *19*, 151.
(34) Packer, K. J.; Poplett, I. J. F.; Taylor, M. J. *J. Chem. Soc., Faraday Trans. 1* **1988**, *84*, 3851.
(35) Cheung, T. T. P. *Phys. Rev. B* **1981**, *23*, 1404.
(36) Stannarius, R.; Schmiedel, H. *J. Magn. Reson.* **1989**, *81*, 339.
(37) Kenwright, A. M.; Packer, K. J. *Chem. Phys. Lett.* **1990**, *173*, 471.
(38) Zhang, S.; Mehring, M. *Chem. Phys. Lett.* **1989**, *160*, 644.
(39) Zhang, S.; Mehring, M. *Chem. Phys. Lett.* **1991**, *176*, 70.
(40) Torchia, D. A. *J. Magn. Reson.* **1978**, *30*, 613.
(41) Strobl, G. R.; Hagedorn, W. *J. Polym. Sci., Polym. Phys. Ed.* **1978**, *16*, 1181.
(42) Glotin, M.; Mandelkern, L. *Colloid Polym. Sci.* **1982**, *260*, 182.
(43) Pranadi, H.; Manuel, A. J. *Polymer* **1980**, *21*, 303.
(44) Draper, N. R.; Smith, H. *Applied Regression Analysis*; Wiley: New York, 1981.
(45) Abragam, A. *The Principles of Nuclear Magnetism*; Oxford University Press: Oxford, UK, 1961; pp 116−8.
(46) Komoroski, R. A. In *High Resolution NMR Spectroscopy of Synthetic Polymers in Bulk*; Komoroski, R. A., Ed.; VCH: Deerfield Beach, FL, 1986; p 121.

(47) Slavicek, E. *Collect. Czech. Chem. Commun.* **1970**, *35*, 2885.
(48) McWhirter, J. G.; Pike, E. R. *J. Phys. A: Math. Gen.* **1978**, *11*, 1729.
(49) Brown, R. J. S. *J. Magn. Reson.* **1989**, *82*, 539.
(50) Whittall, K. P.; MacKay, A. L. *J. Magn. Reson.* **1989**, *84*, 134.
(51) Dectaur, J. D.; Farrar, T. C. *J. Phys. Chem.* **1989**, *93*, 8294.
(52) Clayden, N. J.; Hesler, B. D. *J. Magn. Reson.* **1992**, *98*, 271.
(53) Lin, Y-Y.; Ge, N-H.; Hwang, L-P. *J. Magn. Reson., Ser. A* **1993**, *105*, 65.
(54) Schmidt-Rohr, K.; Spiess, H. W. *Macromolecules* **1991**, *24*, 5288.
(55) Axelson, D. E.; Mandelkern, L.; Popli, R.; Mathieu, P. *J. Polym. Sci. Polym. Phys. Ed.* **1983**, *21*, 2319.
(56) Mandelkern, L.; Peacock, A. J. Studies in Physical and Theoretical Chemistry In Proceedings of an International Course and Conference on the Interfaces between Mathematics, Chemistry, and Computer Science; Lacher, R. C., Ed.; Elsevier: Amsterdam, 1987; Vol. 54, pp 201−227.
(57) Demco, D. E.; Johansson, A.; Tegenfeldt, J. *Solid State Nucl. Magn. Reson.* **1995**, *4*, 13.

MA9516753